Joint Segmentation of 3D Femoral Lumen and Outer Wall Surfaces from MR Images

Eranga Ukwatta[1], Jing Yuan[1], Wu Qiu[1], Martin Rajchl[1], Bernard Chiu[2], Shadi Shavakh[1], Jianrong Xu[3], and Aaron Fenster[1]

[1] Robarts Research Institute, Western University, London, ON, Canada
[2] Department of Electronic Engineering, City University of Hong Kong, Hong Kong
[3] Renji Hospital, Shanghai Jiao Tong University, Shanghai 200127, China
{eukwatta,jyuan,wqiu,mrajchl,afenster}@robarts.ca, bcychiu@cityu.edu.hk

Abstract. We propose a novel algorithm to jointly delineate the femoral artery lumen and outer wall surfaces from 3D black-blood MR images, while enforcing the spatial consistency of the reoriented MR slices along the medial axis of the femoral artery. We demonstrate that the resulting optimization problem of the proposed segmentation can be solved globally and exactly by means of convex relaxation, for which we introduce a novel *coupled continuous max-flow (CCMF) model* based on an Ishikawa-type flow configuration and show its duality to the studied convex relaxed optimization problem. Using the proposed *CCMF model*, the exactness and globalness of its dual convex relaxation problem is proven. Experiment results demonstrate that the proposed method yielded high accuracy (i.e. Dice similarity coefficient $> 85\%$) for both the lumen and outer wall and high reproducibility (intra-class correlation coefficient of 0.95) for generating vessel wall area. The proposed method outperformed the previous method, in terms of computation time, by a factor of ~ 20.

Keywords: Femoral artery segmentation, convex optimization.

1 Introduction

Peripheral arterial disease (PAD) is inflammatory, occluding the arteries with a long term accumulation of plaque. Although PAD may cause morbidity ranging from leg pain to critical limb ischemia, it has long been underestimated and may have been overshadowed by cardio- and cerebro-vascular events and mortality [1,2]. The ankle-brachial index (ABI) is currently used for the diagnosis of PAD, but it is limited in its utility for assessing the progression of the disease and prediction of clinical events. With this regard, MR imaging has been investigated to assess PAD [1] plaque burden and facilitates thickness and volumetric measurements, which are more sensitive to the clinical outcomes than ABI. It is of great interest to efficiently generate an accurate delineation of the femoral lumen and outer wall surfaces (see Fig. 1(a) and (b)) from 3D black-blood femoral MR images (comprising of about 500 - 1000 slices per dataset), which is, however, challenging due to the thin-and-elongated shape of the superficial femoral arteries (SFA) (see Fig. 1(a)) and strong overlapping of the intensity distributions

K. Mori et al. (Eds.): MICCAI 2013, Part I, LNCS 8149, pp. 534–541, 2013.

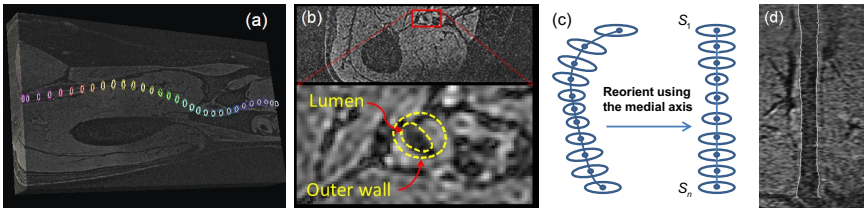

Fig. 1. (a) An example 3D femoral MR image with manual delineations; (b) A transverse slice of a 3D femoral MR image with manual delineations; (c) Reorientation of the femoral MR image using the medial axis of the artery. The reorientation procedure is described in Section 3; and (d) Long axis view of reoriented 3D MR image.

of the outer wall and its surrounding region. Typically, manual segmentation of the femoral lumen and outer wall requires about 80 min [2]. To our knowledge, there is only one study [2] describing a semi-automated segmentation of both the femoral lumen and outer wall surfaces from femoral MR images. Chiu *et al.* [2] proposed a 2D slice-by-slice B-spline snake segmentation procedure, where the segmentation of each slice is propagated as initialization for the subsequent slice to assist segmenting its succeeding slice. Their approach [2] explored sequential segmentation procedures of the femoral lumen and outer wall, which required about 8-10 min of time with extensive user interactions. In addition, such slice-by-slice technique does not globally enforce the inherent spatial coherence of the contours along the medial axis of artery, thus segmentation errors of one slice can be propagated and accumulated in segmentation of its following slices.

Contributions We propose a novel and efficient global optimization-based algorithm to jointly segment the outer wall and lumen of the SFA from 3D black-blood MR images, while globally enforcing the spatial consistency of the re-oriented slice sequence (see Fig. 1(d)) along the medial axis of the artery. We demonstrate that the resulting combinatorial optimization problem can be solved globally and exactly by means of convex relaxation, for which we introduce a new *coupled continuous max-flow (CCMF) model* and present its duality to the studied convex relaxation model. The proposed *CCMF* formulation directly derives a fast dual optimization algorithm.

2 Method

We propose a novel global optimization approach to simultaneously segment the SFA lumen and outer wall surfaces from the input 3D femoral MR image $\mathcal{V}$. Let $\mathcal{S}_1 \ldots \mathcal{S}_n$ be n 2D transverse slices of $\mathcal{V}$ translated along the medial axis of the femoral artery (see Fig. 1(c) and (d) for illustration), where the tubular-like shape of the femoral artery entails spatial consistency along the specified medial axis of the segmented lumen and outer wall regions between every two adjacent reoriented slices. The algorithm simultaneously segments the n MR slices into background, outer wall, and lumen by properly enforcing such prior knowledge.

2.1 Joint Segmentation of Lumen and Outer Wall

Slice-wise Multi-Region Segmentation Model. Let $\mathcal{R}_i^B$, $\mathcal{R}_i^W$ and $\mathcal{R}_i^L$, $i = 1 \dots n$, denote the three regions of background, outer wall and lumen, within the 2D slice $\mathcal{S}_i$, respectively; $u_i^W(x), u_i^L(x) \in \{0,1\}$, $i = 1 \dots n$, be the corresponding indicator labeling functions of $\mathcal{R}_i^W$ and $\mathcal{R}_i^L$. Since the outer wall region $\mathcal{R}_i^W$ contains the lumen region $\mathcal{R}_i^L$ [3](see Fig. 1(b)) within each slice $\mathcal{S}_i$, $i = 1 \dots n$,

$$u_i^L(x) \leq u_i^W(x), \quad \forall x \in \mathcal{S}_i; \quad i = 1 \dots n. \tag{1}$$

The segmentation of each slice $\mathcal{S}_i$, $i = 1 \dots n$, into the three regions of $\mathcal{R}_i^B$, $\mathcal{R}_i^W$, and $\mathcal{R}_i^L$ can be formulated as a coupled continuous min-cut problem [4], which minimizes the following energy function

$$\begin{aligned} E_i(u_i^W, u_i^L) := & \Big\{ \int (1 - u_i^W) C_i^B \, dx + \int (u_i^W - u_i^L) C_i^W \, dx + \int u_i^L C_i^L \, dx \Big\} \\ & + \Big\{ \int_\Omega g_i(x) \left| \nabla u_i^W \right| \, dx + \int_\Omega g_i(x) \left| \nabla u_i^L \right| \, dx \Big\} \end{aligned} \tag{2}$$

over the binary labeling functions $u_i^{W,L}(x) \in \{0,1\}$, subject to constraint (1).

In (2), the functions $C_i^B(x)$, C_i^W, and $C_i^L(x)$ evaluate the cost to label pixel $x \in \mathcal{S}_i$, $i = 1 \dots n$, as the background region $\mathcal{R}_i^B$, the complementary region $\mathcal{R}_i^W \backslash \mathcal{R}_i^L$ and the lumen region $\mathcal{R}_i^L$ respectively; hence, the sum of the first three terms gives the total cost of labeling each pixel with the slice $\mathcal{S}_i$. Moreover, the two weighted total-variation functions of (2) measure the smoothness of the two regions $\mathcal{R}_i^W$ and $\mathcal{R}_i^L$ w.r.t. the labeling functions $u_i^W(x), u_i^L(x) \in \{0,1\}$, where $g_i(x) = \lambda_1 + \lambda_2 \exp(-\lambda_3 |\nabla I(x)|)$ is a function of the image gradient.

Spatial Consistency Prior between Adjacent Slices. The n slices $\mathcal{S}_1 \dots \mathcal{S}_n$ are aligned along the medial axis of the femoral artery (see the blue dotted line in Fig. 1(c)). The tubular shape of the femoral artery enables a strong spatial consistency between every two adjacent slices. With this regard, we propose to enforce such consistency prior of the segmented regions $\mathcal{R}_i^W$ and $\mathcal{R}_i^L$, $i = 1 \dots n$, by penalizing the total spatial differences of the extracted regions between two neighbouring slices, i.e. minimizing

$$\pi_i(u) := \int_\Omega \left| u_{i+1}^W - u_i^W \right| \, dx + \int_\Omega \left| u_{i+1}^L - u_i^L \right| \, dx, \quad i = 1 \dots n-1. \tag{3}$$

Optimization Formulation. In view of (2) and (3), we propose to segment the 3D coupled femoral artery surfaces of the outer wall and lumen by segmenting the n 2D image slices while incorporating inter-slice consistency (3), which can be formulated with a balancing weight $\alpha > 0$ as

$$\min_{u^{L,W}(x) \in \{0,1\}} \sum_{i=1}^{n} E_i(u_i) + \alpha \sum_{i=1}^{n-1} \pi_i(u); \quad \text{s.t. } u_i^L(x) \leq u_i^W(x), \quad i = 1 \dots n. \tag{4}$$

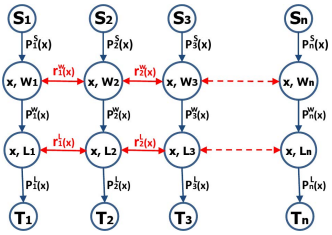

Fig. 2. Flow configurations of the proposed *coupled continuous max-flow model*

2.2 Convex Relaxation and Coupled Continuous Max-Flow Model

In this study, we show that the proposed optimization problem (4) can be globally and exactly solved by its convex relaxation

$$\min_{u^{L,W}(x)\in[0,1]} \sum_{i=1}^{n} E_i(u_i) + \alpha \sum_{i=1}^{n-1} \pi_i(u)\,; \quad \text{s.t. } u_i^L(x) \le u_i^W(x)\,, \quad i = 1\ldots n\,, \quad (5)$$

where the binary-valued constraints $u_i^{L,W}(x) \in \{0,1\}$ in (4) are replaced by their convex relaxation $u_i^{L,W}(x) \in [0,1]$. Note that, (5) amounts to a convex optimization problem with a global optimum. Here, we study (5) by introducing its dual formulation, i.e. the novel *CCMF model*, and show the thresholding of the computed optimum of the convex relaxation problem (5) solves its original combinatorial optimization problem (4) globally and exactly.

Coupled Continuous Max-Flow (CCMF) Model. We introduce the new flow configuration based on the studies in [4] (as illustrated in Fig. 2). For each image slice $\mathcal{S}_i$, $i = 1\ldots n$, we add two image copies Ω_i^W and Ω_i^L w.r.t. the regions $\mathcal{R}_i^W$ and $\mathcal{R}_i^L$; two additional flow terminals: the source s_i and the sink t_i, are added; link the source s_i to each pixel x in Ω_i^W, along which the directed source flow $p_i^s(x)$ is defined; link each pixel $x \in \Omega_i^W$ to the same pixel x at Ω_i^L, along which the directed outer wall flow $p_i^W(x)$ is defined; link each pixel $x \in \Omega_i^L$ to the sink t_i, along which the directed lumen flow $p_i^L(x)$ is defined; within Ω_i^W and Ω_i^L, the local vector flow fields $q_i^W(x), q_i^L(x) \in \mathbb{R}^2$ are given around each pixel x. Between two adjacent Ω_i^W and Ω_{i+1}^W, $i = 1\ldots n-1$, we link $x \in \Omega_i^W$ to the same position $x \in \Omega_{i+1}^W$, along which a coupled flow $r_i^W(x)$ streaming in both directions is defined. Between two adjacent Ω_i^L and Ω_{i+1}^L, $i = 1\ldots n-1$, we link $x \in \Omega_i^L$ to the same position $x \in \Omega_{i+1}^L$, along which a coupled flow $r_i^L(x)$ streaming in both directions is defined.

With the above flow configuration, we introduce the novel *CCMF model*, which maximizes the total flow streaming from the n sources:

$$\max_{p^s,p^t,q,r} \sum_{i=1}^{n} \int_{\Omega} p_i^s(x)\,dx \quad (6)$$

subject to the flow capacity constraints

$$p_i^s(x) \le C_i^B(x)\,, \;\; p_i^W(x) \le C_i^W(x)\,, \;\; p_i^L(x) \le C_i^L(x)\,; \;\; i = 1\ldots n\,; \quad (7)$$

$$\left|q_i^W(x)\right| \leq g_i(x)\,, \quad \left|q_i^L(x)\right| \leq g_i(x)\,; \quad i = 1 \ldots n\,; \tag{8}$$

$$\left|r_i^W(x)\right| \leq \alpha\,, \quad \left|r_i^L(x)\right| \leq \alpha\,; \quad i = 1 \ldots n-1\,; \tag{9}$$

and the flow conservation constraints within each $\Omega_i^{W,L}$, $i = 1 \ldots n$:

$$\rho_1^W(x) := \big(\operatorname{div} q_1^W - p_1^s + p_1^W + r_1^W\big)(x) = 0\,; \tag{10}$$

$$\rho_1^L(x) := \big(\operatorname{div} q_1^L - p_1^W + p_1^L + r_1^L\big)(x) = 0\,; \tag{11}$$

$$\rho_i^W(x) := \big(\operatorname{div} q_i^W - p_i^s + p_i^W + r_i^W - r_{i-1}^W\big)(x) = 0\,; \quad i = 2 \ldots n-1\,; \tag{12}$$

$$\rho_i^L(x) := \big(\operatorname{div} q_i^L - p_i^W + p_i^L + r_i^L - r_{i-1}^L\big)(x) = 0\,; \quad i = 2 \ldots n-1\,; \tag{13}$$

$$\rho_n^W(x) := \big(\operatorname{div} q_n^W - p_n^s + p_n^W - r_{n-1}^W\big)(x) = 0\,; \tag{14}$$

$$\rho_n^L(x) := \big(\operatorname{div} q_n^L - p_n^W + p_n^L - r_{n-1}^L\big)(x) = 0\,. \tag{15}$$

Global and Exact Optimization of (4)**.** By introducing the multiplier functions $u_i^{W,L}(x)$, $i = 1 \ldots n$, to the linear equalities (10) - (15), we then have the equivalent primal-dual model of (6) such that

$$\min_{u^{W,L}} \max_{p,q,r} \sum_{i=1}^{n} \int_\Omega p_i^s(x)\,dx + \sum_{i=1}^{n} \left\langle u_i^W, \rho_i^W \right\rangle + \sum_{i=1}^{n} \left\langle u_i^L, \rho_i^L \right\rangle \tag{16}$$

subject to the flow capacity constraints (7) - (9). By variational analysis, we can prove the following results:

Proposition 1. *The* coupled continuous max-flow model (6)*, the convex relaxation model* (5) *and the primal-dual model* (16) *are equivalent to each other:*

$$(6) \iff (5) \iff (16)\,. \tag{17}$$

Proposition 2. *Let* $(u_1^{W,L}(x), \ldots u_n^{W,L}(x))^* \in [0,1]$ *be the global optimum of the convex relaxation problem* (5)*, the thresholds* $\tilde{u}_i^{W,L}(x) \in \{0,1\}$*,* $i = 1 \ldots n$*, by any* $\gamma \in [0,1)$*, where*

$$\tilde{u}_i^W(x) = \begin{cases} 1\,, & (u_i^W)^*(x) > \gamma \\ 0\,, & (u_i^W)^*(x) \leq \gamma \end{cases}\,,\ \tilde{u}_i^L(x) = \begin{cases} 1\,, & (u_i^L)^*(x) > \gamma \\ 0\,, & (u_i^L)^*(x) \leq \gamma \end{cases} \quad i = 1 \ldots n\,, \tag{18}$$

solves the original combinatorial optimization problem (4) *globally and exactly.*

Coupled Continuous Max-Flow Model. By Prop. 2, the global optimum of the proposed challenging segmentation problem (4) can be achieved by thresholding the optimum of its convex relaxation (5) with any $\gamma \in [0,1)$. However, Prop. 1 shows that the optimum of such convex relaxation problem (5) is given by the optimal multipliers to the corresponding linear equality conditions (10)-(15). Indeed, this directly derives the *CCMF model* based on the the modern augmented Lagrangian algorithm [5,6]; see also [4,7] for detailed algorithmic scheme. The proposed *CCMF algorithm* avoids directly solving the non-smooth function terms in (5) and achieves high efficiency in practice.

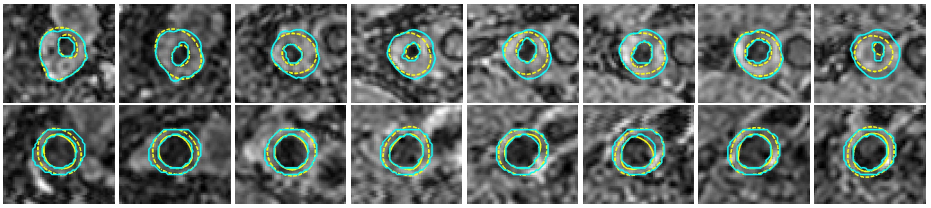

Fig. 3. Slice-wise comparison of the computation results (cyan) to the manual segmentation (yellow) for the femoral wall and lumen boundaries for three 3D MR images

3 Experiments and Results

Segmentation Pipeline. Initially, the user identifies approximately a 300 mm section of the SFA and then samples some seed points on the lumen, outer wall, and background regions in the first and the last slices to generate the corresponding model probability density functions (PDFs) of intensities $Pr(I(x))$, $j = L, W, B$, which are applied to segment the first and last slices using the introduced 2D segmentation algorithm [8]. The 2D segmentations of the first and last slices are further utilized to refine the approximation of the model PDFs for the lumen, outer wall, and background regions of the 3D MR image.

In parallel, an approximate medial axis of the femoral artery is computed to align and reorient the stack of slices for segmentation. Using multi-planar reformatting software, the observer approximately chooses the mid points on transverse cross-sections of the artery with an inter-slice distance of 30 mm (about 11 points in total). These points are then connected by the live-wire algorithm [9], which computes the minimum cost path linking the user-marked points and generates the rest of the points on the medial axis. The Frangi vesselness filter [10] is applied to the 3D MR image and its output is used as the cost map for the live-wire algorithm. The transverse slices are then reoriented along the computed medial axis, as shown in Fig. 1(c) and (d).

The 2D segmentation result of the first slice is used as initialization of the 3D algorithm. We then apply the proposed *CCMF* algorithm to jointly segment the 3D femoral lumen and outer wall surfaces from the reoriented 3D MR image, where the intensity log-likelihood terms [11] $C_i^j(x) = -\ln(Pr(I(x))$, $j = L, W, B$, are used as the data costs of (2). The femoral lumen and outer wall surfaces generated using the algorithm are then mapped to the original space using the inverse transformation, which can be used for further analysis of the vessel wall boundaries. In addition,the parameters (i.e., $\alpha = 18, \lambda_{1,2,3} = 0.1, 1.7, 3$) were optimized sequentially by varying one parameter at a time. The optimized parameters were fixed during the experiments for the entire dataset.

Data and Acquisition. Our data set comprises of ten 3D motion-sensitized driven equilibrium (MSDE) prepared rapid gradient echo sequence (3D MERGE) images from seven subjects. Five of these subjects were symptomatic with intermittent claudication. The MR images were acquired using two stations with

Table 1. Performance results of the proposed algorithm for 10 3D femoral MR images

Metric	DC (%)	AO (%)	MAD (mm)	MAXD (mm)	VWA_{AVG} (mm^2)	VWA_{RMSE} (mm^2)
Wall	89.14±3.70	81.16±3.88	0.44±0.10	0.97±0.23	6.18±5.11	7.8
Lumen	85.43±3.39	80.42±10.74	0.40±0.08	0.87±0.13		

Table 2. Intra-observer variability results of the algorithm using five repetitions of the same observer for 6 femoral MR images

Metric	Lumen	Wall	VWA	Metric	Lumen	Wall	VWA	Metric	Lumen	Wall	VWA
CV(%)	6.43	4.88	6.69	ICC	0.969	0.937	0.949	SD (mm^2)	1.9	2.6	2.3

Table 3. Comparison of the algorithm to Chiu *et al.* [2] using the same data set

	Metric	AO (%)	AD (%)	MAD (mm)	MAXD (mm)	VWA_{AVG} (mm^2)	VWA_{RMSE} (mm^2)
Proposed method	Wall	82.87±4.72	23.54±8.21	0.43±0.13	0.89±0.16	4.77±5.12	6.29
	Lumen	81.35±8.46	24.95±9.32	0.42±0.09	0.86±0.16		
Chiu *et al.* [2]	Wall	84.75±9.46	12.90±12.95	0.32±0.23	0.77±0.52	4.58±7.10	8.45
	Lumen	85.60±9.36	9.77±9.78	0.20±0.17	0.55±0.48		

field-of-view of 400 × 40 × 250 mm to cover up to 500 mm longitudinally with isotropic voxel size of 1.0 mm. The imaging parameters were TR = 10 ms, TE = 4.8 ms, flip angle = 6°, turbo factor = 100 and one excitation (NEX).

Results. The experiments were performed on a Windows PC with a Intel Core i7 CPU and 3GB RAM. The proposed *CCMF* algorithm was implemented in C++ with an interface in Matlab (Natick, MA) and required only 10 s to segment each 3D image, in addition to about 98 s for initialization and pre-processing. The final reconstructed 3D lumen and outer wall surfaces are compared to the manual segmentations on a slice-by-slice basis; some example reconstructed slice-wise results are shown for three subjects in Fig. 3. For the slice-by-slice validation, our data set consisted of 355 2D slices extracted from 10 3D femoral MR images.

To assess the accuracy, we used Dice similarity coefficient (DSC), area overlap (AO), area difference (AD), average and root mean square vessel wall area (VWA) errors [2] and mean and maximum absolute distance errors (MAD and MAXD). Table 1 shows the accuracy evaluation of the proposed algorithm, which yielded a DSC $\geq 85\%$ for both the lumen and outer wall and sub-millimeter errors in MAD and MAXD. The user repeatedly segmented six femoral MR images five times to assess the reproducibility of the algorithm in generating VWA using coefficient of variation (CV), intra-class correlation coefficient (ICC), and standard deviation (SD) (as shown in Table 2). Table 3 shows the comparison of the proposed algorithm to the 2D slice-based method [2] using the same data set. Our algorithm yielded comparably accurate results to [2] while requiring much fewer user interactions and less computation time ($\sim$ 10 s vs. 230 - 290 s).

4 Discussion and Conclusions

Our algorithm yielded high accuracy (i.e. DSC $\geq$ 85% and sub-millimeter error values for MAD and MAXD as shown in Table 1) for the segmentation of both the SFA lumen and outer wall. The algorithm also yielded high reproducibility (i.e. ICC of 0.95 and CV as low as 6.69%) for generating VWA, which is the most important aspect of the algorithm for longitudinal monitoring of PAD plaque burden, because a systematic bias may cancel out when VWA change is measured from baseline to follow-up. The algorithm required much less computing time (10 s vs. 230 - 290 s) and user interactions, comparing to Chiu *et al.* [2], while achieving a comparable accuracy in AO, MAD and MAXD. Currently, most of the observer time is used for identifying the medial axis of the artery, which may be further improved by using an automated centerline detection algorithm.

Acknowledgements. The authors are grateful for the funding support from the Canadian Institutes of Health Research (CIHR) and the Canada Research Chairs (CRC) Program. B. Chiu acknowledges the support of City University of Hong Kong start-up Grant #7200245.

References

1. Isbell, D., Meyer, C., Rogers, W., Epstein, F., et al.: Reproducibility and reliability of atherosclerotic plaque volume measurements in peripheral arterial disease with cardiovascular magnetic resonance. J. Cardiov. Magn. Reson. 9(1), 71–76 (2007)
2. Chiu, B., Sun, J., Zhao, X., Wang, J., Balu, N., Chi, J., Xu, J., Yuan, C., Kerwin, W.: Fast plaque burden assessment of the femoral artery using 3d black-blood mri and automated segmentation. Medical Physics 38, 5370–5384 (2011)
3. Ukwatta, E., Yuan, J., Rajchl, M., Fenster, A.: Efficient global optimization based 3D carotid AB-LIB MRI segmentation by simultaneously evolving coupled surfaces. In: Ayache, N., Delingette, H., Golland, P., Mori, K. (eds.) MICCAI 2012, Part III. LNCS, vol. 7512, pp. 377–384. Springer, Heidelberg (2012)
4. Bae, E., Yuan, J., Tai, X.C., Boycov, Y.: A fast continuous max-flow approach to non-convex multilabeling problems. Technical report CAM-10-62, UCLA (2010)
5. Bertsekas, D.P.: Nonlinear Programming. Athena Scientific (September 1999)
6. Yuan, J., Bae, E., Tai, X.: A study on continuous max-flow and min-cut approaches. IEEE CVPR, 2217–2224 (2010)
7. Yuan, J., Bae, E., Tai, X.-C., Boykov, Y.: A continuous max-flow approach to potts model. In: Daniilidis, K., Maragos, P., Paragios, N. (eds.) ECCV 2010, Part VI. LNCS, vol. 6316, pp. 379–392. Springer, Heidelberg (2010)
8. Ukwatta, E., Yuan, J., Rajchl, M., Tessier, D., Fenster, A.: 3D carotid multi-region MRI segmentation by globally optimal evolution of coupled surfaces. IEEE Transactions of Medical Imaging 32(4), 770–785 (2013)
9. Barrett, W.A., Mortensen, E.N.: Interactive live-wire boundary extraction. Medical Image Analysis 1(4), 331–341 (1997)
10. Frangi, A.F., Niessen, W.J., Vincken, K.L., Viergever, M.A.: Multiscale vessel enhancement filtering. In: Wells, W.M., Colchester, A.C.F., Delp, S.L. (eds.) MICCAI 1998. LNCS, vol. 1496, pp. 130–137. Springer, Heidelberg (1998)
11. Rajchl, M., Yuan, J., Ukwatta, E., Peters, P.: Fast interactive multi-region cardiac segmentation with linearly ordered labels. In: IEEE ISBI, pp. 1409–1412 (2012)